Physica B 171 (1991) 185–189
North-Holland

Correlation between magnetism and local order: The case of the mixed valent system $CeFe_2$

A. Marcelli[a], J. Chaboy[b], J. Garcia[b] and F. Sette[c]

[a]*INFN Laboratori Nazionali di Frascati, 00044 Frascati, Italy*
[b]*Instituto de Ciencia de Materiales de Aragón, CSIC-Universidad de Zaragoza, 50009 Zaragoza, Spain*
[c]*AT&T Bell Laboratories, Murray Hill, NJ 07974, USA*

This work is an extensive study of the cubic Laves phase rare earth compounds: $CeFe_2$ and its related hydrides performed by X-ray absorption spectroscopy. The $CeFe_2$ system has been investigated by Extended X-ray Absorption Fine Structure (EXAFS) both at cerium and iron sites and by X-ray Absorption Near Edge Spectroscopy (XANES) at different edges of both cerium and iron atomic species. Attempts to relate magnetic properties of this system with the electronic properties and the crystal structure of the disordered hydridate phases have been performed.

1. Introduction

The $CeFe_2$ crystallizes in the cubic $MgCu_2$ structure with lattice constant $a = 7.304$ Å, and is a ferromagnetic system with a Curie temperature of $T_C = 235$ K [1–3]. The presence of hydrogen in the host metal lattice produces marked changes in the physical properties of rare earth transition metal systems. In particular, the effect of the hydrogen absorption in $CeFe_2$ is to increase the magnetic ordering temperature and the magnetization [4]. The value of saturation magnetization for $CeFe_2H_{3.75}$ is about $2.1\mu_B$/Fe which is about 70% higher than the original intermetallic compound and the Curie temperature ($T_C = 358$ K) is 60% higher than $CeFe_2$ [3]. These changes are induced by the distortion of the crystal structure and the modification of the electronic configuration of the system. This work correlates the magnetic properties of $CeFe_2$ after hydridation, with the structural and electronic information derived from X-ray absorption spectroscopy (XAS) experiments [5]. In fact, selecting the energy of the initial state, XAS gives direct information about the partial and local empty DOS of the final state, via the dipole selection rule [6, 7].

The X-ray absorption investigation has been carried out on $CeFe_2$, $CeFe_2D_{2.8}$ and $CeFe_2H_{3.75}$ compounds. Both EXAFS and XANES at the L_1, L_2 and L_3 cerium edges and at the K iron edge have been measured. Discussion of the complementary information given by this data is necessary to get a description of the electronic and structural changes which occur during the hydridation process.

2. Experimental

Several samples were measured in different experimental runs at the PULS Synchrotron Radiation Facility of Frascati. The procedure of preparation of these materials and their characterization is described elsewhere [8]. Absorption spectra in the X-ray range were carried out at room temperature, in the transmission mode, using a Si (1 1 1) double crystal monochromator. The experiments at the L_{23} edge of iron were performed at the Brookhaven Synchrotron Radiation Line using the DRAGON monochromator [9, 10]. For the photoabsorption experiments, materials were loaded into the vacuum chamber without bake-out. Spectra were recorded in this energy range by monitoring the total electron yield.

3. Results and discussion

The understanding of the mechanisms leading to the formation of local magnetic moments of 3d atoms in metallic hosts is a key problem of magnetism. The magnetic behavior in d metal hosts is governed by the interatomic interactions of 3d with other d band electrons. Indeed in RM_2 systems (R = rare earth, M = transition metal) the M-3d states and R-5d states strongly hybridize to form bonding and antibonding states [11, 12]. However, self-consistent energy-band calculations have demonstrated that the inclusion of 3d–4f hybridization in $CeFe_2$ is essential to yield the correct total moment ($2.4\mu_B$/formula unit) and to explain the anomaly of the lattice constant [11].

A comparison of K-iron edge in $CeFe_2$ and in $CeFe_2H_x$ at the highest hydrogen concentration, is shown in fig. 1. It indicates that the hydridation process leads to a decrease of the hybridization between the empty p final states around the iron site and the Fe-3d states, however no shift of the Fermi energy occurs. The difference between the normalized spectra of $CeFe_2$ and $CeFe_2H_{3.75}$ shows, in fact, two pronounced peaks: one at the edge (~7101 eV) and one at higher energy (~7113 eV). The first one indicates a decrease of the hybridization after the hydrogen absorption. Indeed as the hydrogen concentration increases, more valence electrons are available and a progressive filling of the 3d dominated band takes place, decreasing the mixing between 3d and sp band states. The second peak is assigned to a multiple scattering resonance produced by structural distortion of the atomic cluster around the iron atom.

Figure 2 shows the Fe-L_{23} spectra for $CeFe_2$ and $CeFe_2H_{3.75}$. The 2p level spectra are split by the spin–orbit coupling into two major contributions: the transition from the $2p_{3/2}$ core level to the unoccupied 3d levels (L_3) and, at higher excitation energies, that from the $2p_{1/2}$ level (L_2). In spite of the general complexity of these spectra which is governed by the interplay between the crystal field potential and the different spin–orbit and spin–spin coupling mechanisms of the 2p holes and the 3d electrons, the multiplet structure in these compounds is essentially a single doublet as observed in other transition metal systems [13]. Calculations to reproduce the experimental data are necessary to determine the weight of the various coupling schemes. However, looking only at the lineshape of the L_{23} spectra, we have qualitative evidence that the crystal symmetries around the iron site for the two phases are the same. In fact, both spectra, which are mainly due to the dispersion of the

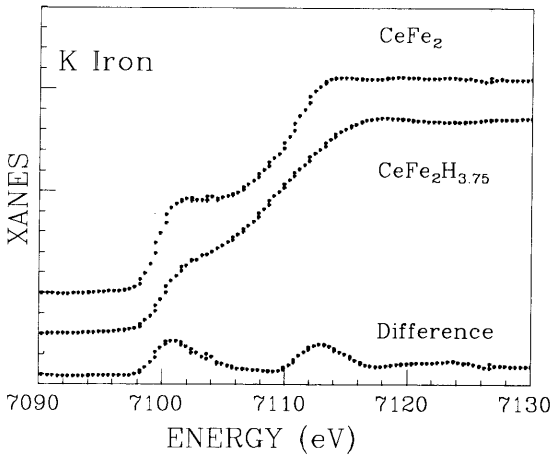

Fig. 1. Comparison of the K edge of iron in $CeFe_2$ and $CeFe_2H_{3.75}$. The lower curve is the difference between the two iron spectra.

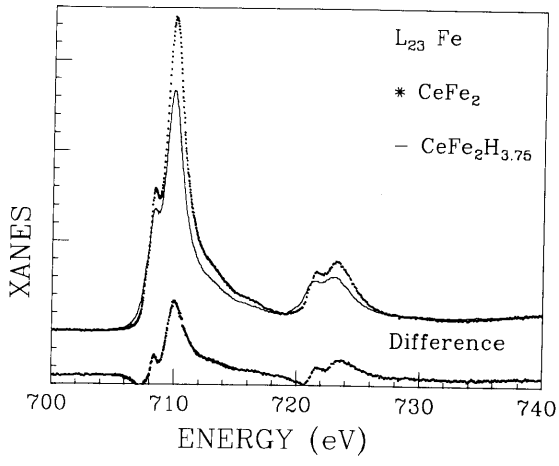

Fig. 2. Comparison of the L_{23} edge of iron in $CeFe_2$ and $CeFe_2H_{3.75}$. The lower curve is the difference between the two iron spectra.

empty 3d bands, are very similar with the only appreciable difference being the global decrease of the intensity of the hydridate spectrum. This reduction is attributed to a decrease of both localized and delocalized densities of d empty states at the iron site. Moreover, the slope at the onset of the edge, which reflects the position of the Fermi level in the metal is slightly changed with a small tail that appears at the low-energy side both at the L_3 and L_2 edges. In agreement with the K edge results, no appreciable shift of the Fermi energy can be detected at the L_{23} edges.

These observations indicate that electrons added to the system, by the hydrogen fill localized 3d valence states at the iron site. This phenomenon can be visualized using a rigid band model, where the iron 3d band moves down.

Hydridation effects on the local structure around the iron site, were primarily investigated by Fe K-EXAFS. Figure 3 (left panel) shows a comparison between the EXAFS signals in these compounds. Clearly the reduction of the signal indicates an increase of the structural disorder around the iron due to the increase of the concentration of hydrogen. Additional information on this process can be obtained from fig. 3 (right panel) where the Fourier transform of the signals are reported.

The coordination of the first shell of iron ions remains unchanged in the highest hydridate phases, while the second coordination shell of cerium practically disappears. In the framework of a multiple scattering theory, XANES spectra give additional evidence of the lack of local order. In fact, the second peak in the difference spectra of fig. 1 can be attributed to a decrease of the local order of the first coordination sphere and to a loss of order beyond the first shell [14]. Additionally, EXAFS analysis is in agreement with the L_{23} indication concerning the d symmetry observed at the iron site.

The analysis of the cerium X-ray absorption data is more complicated, due to the presence of a mixed valent state. L_3 XANES spectra of mixed valence compounds are generally analyzed by deconvolution using arctangent functions to describe the continuum and Lorentzian functions for the $4f^n$ atomic localized states. From this analysis an approximate 4f electronic occupation can be deduced [14, 15]. The Ce-L_3 spectra of these compounds, reported in fig. 4 (left panel),

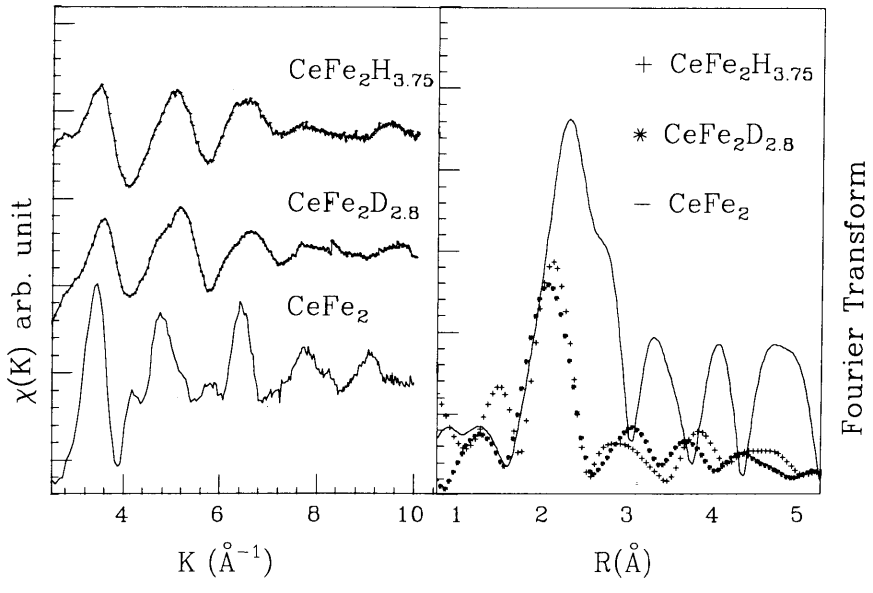

Fig. 3. Iron K EXAFS spectra of $CeFe_2$ and its hydridates (left panel) and their Fourier transform (right panel).

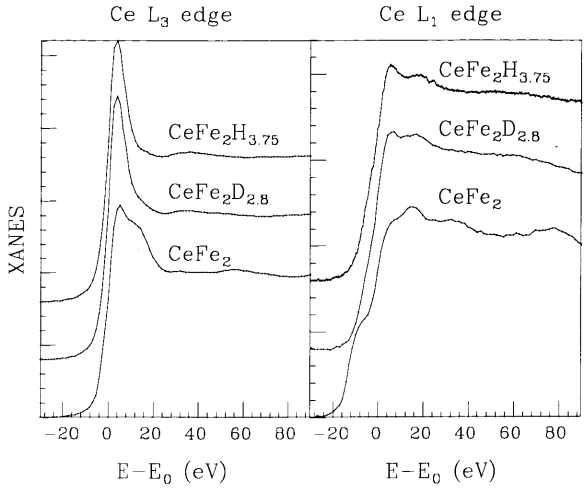

Fig. 4. Cerium L_3 (left panel) and L_1 (right panel) XANES spectra of the $CeFe_2$ and its hydridates.

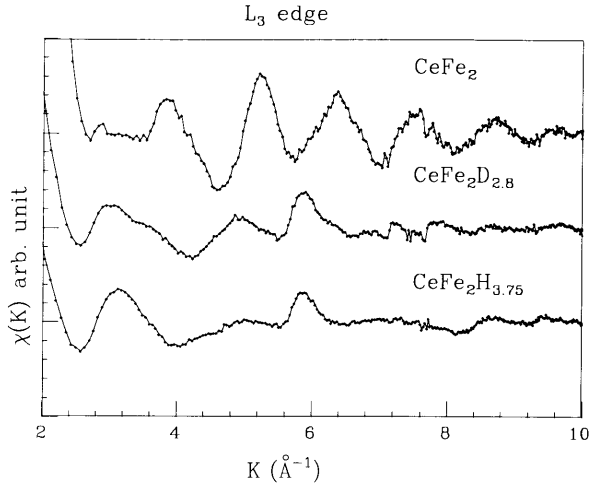

Fig. 5. Ce L_3 EXAFS spectra of the $CeFe_2H_x$.

show that hydrogen induces the suppression of the mixed valence state as observed in other systems, e.g., $CeNi_2H_x$ [16]. The $4f^1$ electronic occupation is then raised by hydrogen absorption. (Similar behavior is observed at the Ce-L_2 edge.) In the case of $CeFe_2$, the L_1 spectrum displayed in fig. 4 (right panel) exhibits at the edge a double staircase feature split by about 8 eV, which should be attributed to the presence of the mixed valance state in analogy to the L_3 edge [17]. Hydridation of CeF_2 suppresses this structure, reflecting the change of the p-projected density of the conduction band and is in agreement with the Fe K edge data. This change can be correlated with the L_3 spectrum, which shows only one white line, indicating the presence of a Ce 3^+ valance state [18]. Both the L_1 and the L_3 data of Ce in the hydridate phases resemble data for atomic cerium, supporting the indication of a reduction of rare earth hybridization [19].

L_3 Ce EXAFS spectra of the $CeFe_2$ and their hydridates are shown in fig. 5. These data show that hydrogen breaks down the periodicity of the rare earth sublattice and supports a strong reduction of the local order at the cerium site. However, it is not possible to establish the details of the final phase of the hydridation process. In fact the structural disorder induced by hydridation, smears out the EXAFS oscillatory signal, but the residual oscillations indicate that there remains a defined distribution of atoms around cerium [18].

The description derived from this XAS investigation assigns the increase of the magnetic moment as caused essentially an electronic dynamic induced by hydrogen. Although the details of the process are not completely clear, this mechanism destroys the Fe–Ce hybridization.

The role of the structural disorder appears weak around iron, while it is significant around the cerium site. This last observation raises the question of whether a boot strapping effect in this magnetic alloy (and/or in other binary alloys) exists, in the sense that induced magnetism for iron (one site) enhances the magnetism of the cerium (at an another site). As a consequence, the magnetism of Ce can be induced by the suppression of the 4f hybridization with 3d electrons, which increases the local moment on the Ce site [11], and by the correlated change of 3d–5d hybridization determined by structural disorder effects.

Acknowledgements

This work was partially supported by the agreement INFN-CICYT and by Spanish CICYT

Proj. Nr. MAT 88–0302. We would like to thank D. Fruchart and S. Miraglia who provided us the samples.

References

[1] R.C. Mansey, G.V. Raynor and I.R. Harris, J. Less-Common Metals 14 (1968) 329.
[2] K.H.J. Buschow and J.S. van Wieringen, Phys. Status Solidi 42 (1970) 231.
[3] A.M. van Diepen and K.H.J. Buschow, Solid State Commun. 22 (1977) 113.
[4] K.H.J. Buschow and R.C. Sherwood, J. Appl. Phys. 49 (1978) 1480.
[5] X-Ray Absorption: Principle, Applications, Techniques of EXAFS, SEXAFS, XANES, R. Prinz and D. Koningsberger, eds. (Wiley, New York, 1988).
[6] A. Balzarotti, M. De Crescenzi and L. Incoccia, Phys. Rev. B 25 (1982) 6349.
[7] I. Davoli, A. Marcelli, G. Fortunato, A. D'Amico, C. Coluzza and A. Bianconi, Solid State Commun. 71 (1989) 383.
[8] J. García, J. Bartolomé, M. Sanchez del Rio, A. Marcelli, D. Fruchart and S. Miraglia, Z. Phys. Chem., Wiesbaden (Germany) 163 (1989) 277.
[9] C.T. Chen and F. Sette, Rev. Sci. Instrum. 60 (1989) 1616.
[10] F. Sette and C.T. Chen, Nuovo Cimento 25 (1990) 363.
[11] O. Eriksson, L. Nordström, M.S.S. Brooks and B. Johansson, Phys. Rev. Lett. 60 (1988) 2523.
[12] S.N. Mishra, K.D. Gross, L. Büermann, M. Luszik-Bhadra and D. Riegel, Phys. Rev. Lett. 63 (1989) 2594.
[13] S. Sugano, Y. Tanabe and H. Kamimura, Multiplets of Transition-Metal Ions in Crystals (Academic, New York, 1970).
[14] J. García, A. Marcelli, M. Sanchez del Rio, J. Bartolomé, D. Fruchart, S. Miraglia and F. Vaillant, Physica B 158 (1989) 521.
[15] J. Röhler, in: Handbook on the Physics and Chemistry of Rare Earths, Vol. 10, K.A. Gschneidner and S. Hüfner, eds. (Elsevier, Amsterdam, 1987).
[16] V. Paul-Boncour, M. Diaf, A. Percheron-Guegan and J.C. Achard, J. Phys. (Paris) C 8 (1986) 1093.
[17] A. Marcelli and A. Bianconi, Physica B 158 (1989) 529.
[18] J. Chaboy, J. Carcía, J. Bartolomé, D. Fruchart, S. Miraglia and A. Marcelli, Nuovo Cimento 25 (1990) 777.
[19] G. Materlik, B. Sonntag and M. Tausch, Phys. Rev. Lett. 51 (1983) 1300.